Bull. Nov. Comp. Center, Math. Model. in Geoph., 20 (2017), 57–66

The simulation of the 16 September 2015 Chile (Illapel) tsunami source by the inversion of tsunami waveforms

T.A. Voronina, V.V. Voronin, A.V. Loskutov

Abstract. An application of the original numerical inversion technique to modeling the tsunami sources of the 16 September 2015 Chile tsunami is presented. The problem of recovering a tsunami source from remote measurements of the incoming wave in the deep-water tsunameters is considered as an inverse problem of mathematical physics in the class of ill-posed problems. This approach is based on the least squares and the truncated singular value decomposition techniques. As is done in the inverse seismic problem, the numerical solutions obtained by mathematical methods become unstable due to the presence of noise in real data. The method proposed suppresses the negative effect of the ill-posedness of the problem determining the inevitable instability of the numerical solution. Implementation of the methodology proposed to the 16 September 2015 Chile tsunami has successfully produced the tsunami source model. The tsunami source recovered by the method proposed can find practical applications both as an initial condition for various optimization approaches and for computer-aided calculation of the tsunami wave propagation.

1. Introduction

The mega thrust earthquakes quite often result in large tsunamis that may inflict a severe loss and pain to the population of the coastal communities. The development of the Tsunami Warning Systems is likely to be the most constructive way in the mitigation of the destructive effect of potential tsunamis. The key point in the state-of-the-art in the tsunami forecasting is constructing a reliable tsunami source.

In this paper, the problem of recovering a tsunami source from available measurements of the incoming wave is considered as an inverse problem of mathematical physics. It is well-known that such problems belong to the class of ill-posed or conditionally well-posed ones. This imposes severe constraints on the observational system and the mathematical apparatus employed for solving the problem.

A formal inversion method proposed by Satake in [1] is currently widely used [2–4]. This method is based on the linear theory and the seismological information about the source is extensively used. The possibility of using a nonlinear theory of wave propagation appeared in the adjoint method firstly proposed by Pires and Miranda in [5]. This method based on the op-

timization approach is also often used to solve the inverse tsunami problem. However, the use of an optimization approach in geophysical applications is associated with considerable difficulties: choosing an initial approximation; studying the existence, uniqueness, and stability of a target functional minimum point; and the need to solve the direct problem many times. Recently, the NOAA (USA) has successfully used a method of minimum residuals [6–8] when, on the basis of well-known models, the source shape is determined from wave heights coinciding at certain points.

In the present paper, the tsunami wave propagation is considered within the scope of the linear shallow-water theory. The wave run-up processes of on the shore structures are not taken into account. A function of the water surface elevation relative to the mean sea level is considered to be a solution of the linear shallow-water equations

$$\eta_t + g\nabla \cdot (h\vec{V}) = 0, \qquad \vec{V}_t + g\nabla\eta = 0 \tag{1}$$

completed by the following initial conditions

$$\eta|_{t=0} = \varphi(x, y), \qquad \vec{V}|_{t=0} = 0 \tag{2}$$

and the boundary conditions

$$\vec{V} \cdot \vec{n} = 0 \qquad \text{on the solid boundary,} \tag{3}$$

$$-c\vec{V} \cdot \vec{n} - \eta_{tt} + \frac{c^2\partial^2\eta}{2\partial\vec{\tau}^2}\Big|_\Gamma = 0 \qquad \text{on the open boundary.} \tag{4}$$

In the above equations, the vector $\vec{V} = (v_x, v_y)$ is the horizontal fluid velocity vector whose x- and y-components are, respectively, v_x and v_y; $h(x, y)$ is the water depth; g is the gravity acceleration; $c(x, y) = \sqrt{gh(x, y)}$ is the wave phase velocity; $\vec{n}$ and $\vec{\tau}$ are the outwardly directed unit vectors, normal and tangential to the boundary, respectively; $\varphi(x, y)$ is the initial water displacement defined in the tsunami source area $\Omega : \{(x, y) \in [0, l_1] \times [0, l_2]\}$.

The inverse problem in question is to infer the unknown initial water displacement $\varphi(x, y)$ as data output, while the observed tsunami waveforms as data input are assumed to be known on a set of points $M = \{(x_p, y_p), p = 1, \ldots, P\}$:

$$\eta(x, y, t) = \eta_0(x, y, t), \quad (x, y) \in M.$$

An unknown initial tsunami waveform (below called *tsunami source*) is represented as a part of a spatial harmonics series $\{\varphi_{mn}(x, y)\}$ in the source area Ω:

$$\varphi(x, y) = \sum_{m=1}^{I}\sum_{n=1}^{J} c_{mn}\varphi_{mn}, \qquad \varphi_{mn} = \sin\frac{m\pi x}{l_1}\sin\frac{n\pi y}{l_2}, \tag{5}$$

with unknown coefficients $\vec{c} = \{c_{mn}\}$. In our case, the inverse problem data are the observed waveforms (*marigrams*) $\vec{\eta}_0$ known on a set M and at time instants t_j, $j = 1, \ldots, N_t$. Then the vector $\vec{\eta}_0$ containing the observed tsunami waveforms is expressed as follows:

$$\vec{\eta}_0 = \boldsymbol{A}\vec{c}, \tag{6}$$

where $\boldsymbol{A}$ is a matrix whose columns consist of computed waveforms for every spatial harmonic $\varphi_{mn}(x, y)$ used as initial condition to the direct problem (1)–(4). An original method for recovering a tsunami source based on the inversion of remote measurements of the water-level data without a priori information on a source but on their general spatial localization have been developed. In this method, the inverse problem operator was regularized by the least square inversion using the truncated Singular Value Decomposition approach and the r-solution method were described in their fundamentals in previous papers [9–12].

As a result of the numerical process, the so-called r-solution is a projection of the exact solution onto a linear span of r first right singular vectors $\{\vec{e}_j\}$ corresponding to the largest singular values of a compact operator of the direct problem:

$$\varphi^{[r]}(x, y) = \sum_{j=1}^{r} \alpha_j \vec{e}_j,$$

where $\alpha_j = \dfrac{(\vec{\eta}_0, \vec{l}_j)}{s_j}$, $\vec{l}_j$ and $\vec{e}_j$ are the left and the right singular vectors of the matrix $\boldsymbol{A}$ and s_j are its singular values. We use a value of $\operatorname{cond} \boldsymbol{A}^{[r]} = s_1/s_r$ as a criterion for selection r. In all experiments below r was selected to match the equality $\operatorname{cond} \boldsymbol{A}^{[r]} \approx 100$.

The properties of the obtained r-solution are defined largely by the properties of the inverse operator that were numerically investigated in [13]. The location of tsunami waveforms recorders (bellow called *receivers*) affects the choice of number r by such a way: the better is the configuration of the observational system the longer is a weakly decreasing part of the spectrum. The number r is taken to be much smaller than the minimal dimension of the matrix. It is natural that, as r increases, the amount of information on the obtained r-solution also increases, but the stability decreases.

As in all inverse seismic problems, the numerical solutions obtained by mathematical methods become unstable due to the presence of noise in real data. The method of r-solutions makes it possible to avoid instability in the solution to the ill-posed problem under study. Setting a certain condition number $\operatorname{cond} \boldsymbol{A}^{[r]}$ of the finite-dimensional system matrix, we can determine a possible number r from the relation $r = \max\{k : \ s_1/s_k \leq \operatorname{cond} \boldsymbol{A}^{[r]}\}$.

Finally, r is determined by the behavior of the singular spectrum and the noise level in the data that are determined by the observational system and bathymetry.

As it was shown in [11], analyzing the singular spectra of the matrices obtained in the course of numerical calculation one can estimate the future inversion by a certain observational system that would allow offering a more effective disposition for the tsunami wave recorders by precomputations. The method proposed seems to be attractive from the computational stand point since the main efforts are required only once for calculating the matrix whose columns consist of computed waveforms for each harmonic as a source.

The focus of this research is on the study of the number of the spatial harmonics used in the form of the solution on the inversion result. The results of numerical experiments are presented in the case study of the 16 September, 2015, Chile (Illapel) tsunami.

2. Application to the Chile Tsunami case of September 16, 2015

A tsunami is being formed when the seafloor is suddenly raised or lowered. The most destructive tsunamis are formed by the occurrence of large earthquakes, with epicenters located on the deep ocean floor. These usually occur in the earths regions characterized by high seismic activities due to the collision of two plates along tectonic boundaries. This phenomenon is the cause of many earthquake tsunamis that repeatedly happen offshore Chile, where the Nazca plate subducts beneath the South American plate having generated tsunamis. The latter have caused damage not only on the Chilean coast but also across the Pacific Ocean.

The 2015 Illapel earthquake occurred at 22:54:32 (UT) on 16 September, at 31.573° S, 72.674° W at 22.4 km depth (according to the United States Geological Survey). This earthquake as well as the associated tsunami have been studied by many researchers from various aspects allowing them to design slightly different models of the earthquake source based on the various geophysical data: near-field seismograms, teleseismic waveforms and back projections, GPS and InSAR data, and tsunami waveforms [14]. There has also been determined a tsunami source area, approximately, 70 km to the NW of the epicenter by the method of the backward ray tracing of the observed tsunamis [14]. The distribution of tsunami heights was assumed to be consistent with the slip distribution, their maxima vary from 4 m to 12 m.

In this study, the inversion method described above was applied to the 2015 Illapel event to recover the tsunami source by the inversion of the tsunami waveforms recorded only by the Deep-ocean Assessment and Reporting of Tsunamis (DART®) buoys.

The simulation domain is the water part of the rectangle $\Pi = \{(x, y) : 102^\circ\,\mathrm{W} \le x \le 70^\circ\,\mathrm{W},\ 12^\circ\,\mathrm{N} \le y \le 38^\circ\,\mathrm{S}\}$. It is covered by a 1-minute grid of 1921×3001 points to follow GEBCO bathymetry (http://www.gebco.net/).

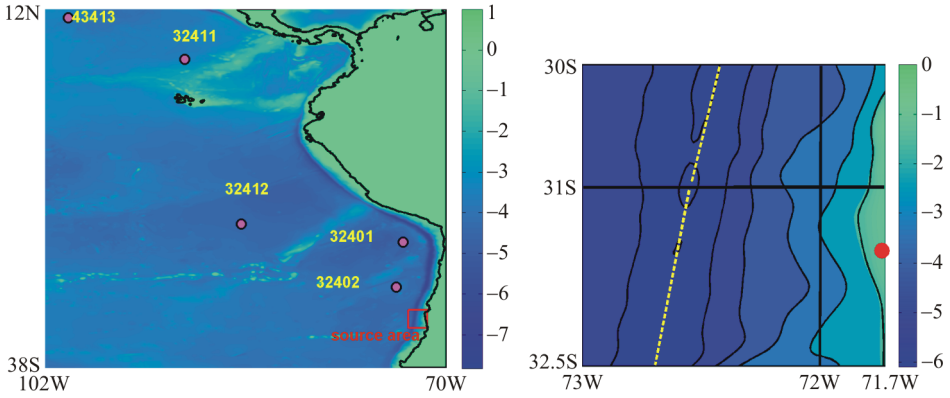

Figure 1. The bathymetry in calculation domain Π: the black line corresponds to 0-level of the depth (in km). The axis X is Longitude, the axis Y is Latitude, the axis Z is the depth. DART® buoys are marked by the magenta circles with numbers and the target domain is marked by the red rectangle. The target domain Ω is marked with the "levels" line, the epicenter of earthquake is marked by the red circle, the yellow dashed line corresponds to trench axis

The source area is assumed to be $\Omega = \{71.6^\circ\,\mathrm{W} \le x \le 73^\circ\,\mathrm{W},\ 30^\circ\,\mathrm{S} \le y \le 32.5^\circ\,\mathrm{S}\}$. It is covered by a grid of 77×151 points. The DART® data are provided by the National Oceanic and Atmospheric Administration (NOAA) of the United States (http://www.ndbc.noaa.gov/dart.shtml). At the coastal boundaries of the calculation domain, conditions of full reflection, as well as at the open sea boundaries, the wave permeable conditions are formulated. The time step $\Delta t = 4$ s, and the length of each marigram part being used $N_t = 1001$, beginning with the first arrival of the wave at the corresponding receiver. An observational system consists of five deep-water DART® recorders numbered counterclockwise as shown in Figure 1: 1 — 32402, 2 — 32401, 3 — 32412, 4 — 32411, and 5 — 43413.

The original code is used to numerically simulate the tsunami propagation. It is a FORTRAN code based on a finite difference algorithm using an explicit-implicit difference scheme constructed with a four-point stencil on a uniform rectangular staggered grid [15], which solves the linear shallow water equations. The scheme is second-order approximation in space and first-order approximation in time. Let us assume that the tsunami wave excitation is caused by an abrupt rising and sinking of the bottom at the initial time from a state of rest, and that the water surface is similar to the bottom shape in the tsunami source area.

First, the proposed algorithm was tested with the synthetic source and with the calculation domain of the real Chile offshore bathymetry. The synthetic marigrams were calculated at the same nodes where the real DARTs are located. In the case study with the synthetic waveforms, we obtain syn-

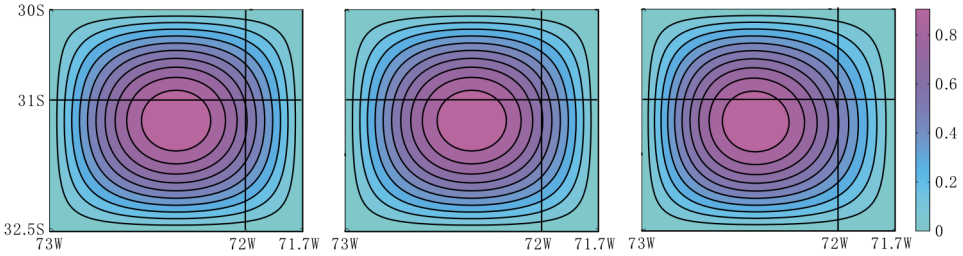

Figure 2. The initial water displacement equal to the first harmonic $\varphi(x, y) = \varphi_{11}$ in the domain Ω (left); the recovered function obtained by use of all five available synthetic waveforms calculated at the nodes of receivers $\{1, 2, 3, 4, 5\}$ (middle, $\varphi_{\max} = 1.07$ m, $\varphi_{\min} = -0.003$ m, $I = J = 4$); and the recovered function obtained by use of three waveforms calculated at the nodes of receivers $\{1, 2, 3\}$ (right, $\varphi_{\max} = 0.99$ m, $\varphi_{\min} = 0$ m, $I = J = 2$). In both calculations cond $\boldsymbol{A}^{[r]} \approx 100$

thetic *marigrams* in all the receivers by solving the forward problem (1)–(3) with appropriate boundary conditions and with the first spatial harmonic determined in (5) in the source area as a source: $\varphi_{\max} = 1.0$ m; $\varphi_{\min} = 0$. This initial water displacement is plotted in Figure 2 on the left. Thus, the vector $\overline{\eta}_0(x, y, w)$ was calculated by means of equation (6). The recovered functions are plotted in Figure 2 in the middle and on the right.

In Figure 3 one can compare the synthetic "observed" (the black line) tsunami waveforms and the calculated ones with five synthetic marigrams as the input data at the nodes of the receivers $\{1, 2, 3, 4, 5\}$ (the blue line) as well as the marigrams obtained as a result of the inversion based on three waveforms calculated on the set of points corresponding to receivers $\{1, 2, 3\}$ (the red line). The lengths of the waveforms equal to 80 min and 40 min, respectively. All calculated waveforms have a good matching with the synthetic "observed" ones. This indicates to an inessential influence of the presence of receivers 4 and 5 on the results of the inversion. The number of used spatial harmonics is defined by the simple shape of synthetic source in this case. These experiments have confirmed the validity of the proposed method.

Further, we switched from the numerical experiments with synthetic data to the fully real set-up with observed data measurement by the above mentioned DART® buoys.

In Figure 4, the number of spatial harmonics is varied according to formula (5). The accuracy of the shape recovered depends on the number of spatial harmonics used. This parameter could be defined by the way of evaluating the coefficients of the singular vectors of the matrix $\boldsymbol{A}$ by the spatial harmonics.

It is clear that each harmonic on a given bathymetry is recovered with its own error. Therefore, the results of the inversion, in addition, depends

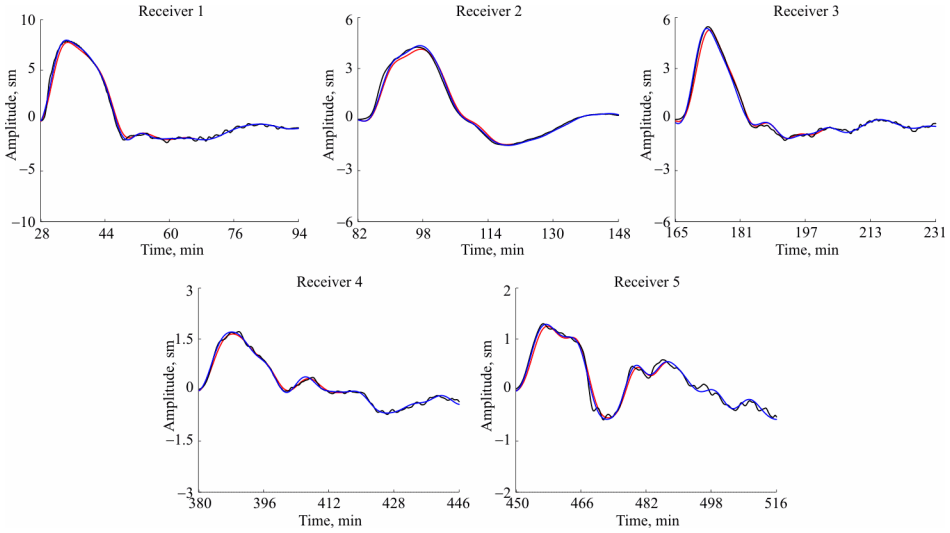

Figure 3. Comparison of the synthetic "observed" tsunami waveforms (the black line) with the calculated ones based on the inversion with five available synthetic waveforms (the blue line, $I = J = 4$) and the ones based on the inversion with three waveforms obtained in the nodes corresponding to the receivers $\{1, 2, 3\}$ (the red line, $I = J = 2$)

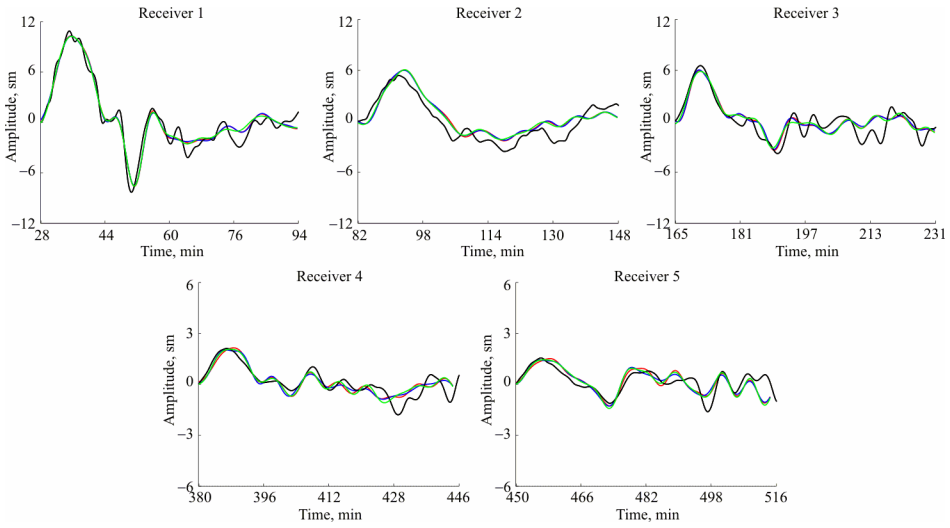

Figure 4. Comparison of the observed tsunami waveforms (the black line) with the calculated ones using the marigrams of receivers $\{1, 2, 3, 4, 5\}$ (the blue line, $I = J = 8$) and the ones based on the inversion with three tsunami waveforms recorded by receivers $\{1, 2, 3\}$ (the red line, $I = J = 8$). The green line corresponds to the case of the inversion based on five marigrams and $I = J = 7$

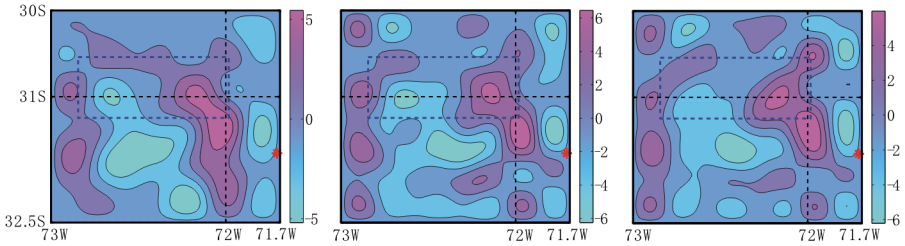

Figure 5. The recovered tsunami sources in the target domain inverted by the marigrams observed on the set of the receivers $\{1, 2, 3, 4, 5\}$ with different numbers of harmonics used: $I = J = 7$, $\varphi_{\max} = 7.6$ m, $\varphi_{\min} = -5.2$ m (left), $I = J = 8$, $\varphi_{\max} = 9.01$ m, $\varphi_{\min} = -6.3$ m (middle), and on the set of the receivers $\{1, 2, 3\}$ with $I = J = 8$, $\varphi_{\max} = 7.4$ m, $\varphi_{\min} = -6.2$ m (right). In all calculations $\operatorname{cond} \boldsymbol{A}^{[r]} \approx 100$. The blue dashed line indicates the inferred tsunami source

on a set of harmonics used. The number of required harmonics in the representation of the desired function is also determined by the heterogeneity of the ocean bottom topography in the direction of the axis OX (horizontal) and the axis OY (vertical), respectively. In the course of the numerical simulation conducted it was revealed that the low-frequency harmonics in the direction of the axis OX corresponding to $\{I = 1, \ldots, 8\}$ in combination with the harmonics with respect to $\{J = 1, \ldots, 8\}$ are recovered sufficiently well. The use of a set of the high-frequency harmonics along the axes OX and OY, which are recovered essentially worse, leads to deterioration in the result of the recovery of the marigrams at the desired points in the simulation domain. Comparison between Figures 5 left and middle as well as by the corresponding marigrams in Figure 4 confirm such inference. In addition, comparing Figures 5 middle and right, we can conclude that the "contribution" of data received from the remote receivers numbered as 4 and 5 is inessential as in the case of the abovementioned test for the recovery of the first harmonic. It is especially important, that the calculated and observed real tsunami waveforms coincide well in all the receivers including those numbered as 4 and 5.

Conclusion

The instability of a numerical solution of the ill-posed inverse problem in question in many ways is due to the noise in real marigrams that is a common feature in any real application. The approach based on r-solution method allows one to control the instability of a numerical solution and to obtain an acceptable result in spite of ill-posedness of the problem. The method seems attractive from the computational point of view since the main efforts are required for calculating matrix $\boldsymbol{A}$. If an observational system is fixed and tsunami-prone areas are defined, one can compute the matrix only once

as a preliminary stage. The method makes it possible to obtain tsunami waveforms at the points where there are no observed ones as well simultaneously with the determination of the source shape and its localization. The results of the numerical experiments are in good agreement with the results obtained from seismic data by other researchers.

Acknowledgements. The author would like to thank Dr. A.A. Romanenko for his help in carrying out the calculations.

References

[1] Satake K. Inversion of tsunami waveforms for the estimation of hereogeneous fault motion of large submarine earthquakes: the 1968 Tokachi-oki and the 1983 Japan sea earthquake // J. Geophys. Res. — 1989. — Vol. 94. — P. 5627–5636.

[2] Baba T., Cummins Ph.R., Hong K.Th., Tsushima H. Validation and joint inversion of teleseismic waveforms for earthquake source models using deep ocean bottom pressure records: a case study of the 2006 Kuril Megathrust Earthquake // Pure and Applied Geophysics. — 2009. — Vol. 166, No. 1–2. — P. 55–76.

[3] Tsushima H., Hino R., Tamioka Y., et al. Tsunami waveform inversion incorporating permanent seafloor deformation and its application to tsunami forecasting // J. Geophys. Res. — 2012. — Vol. 117. — B03311. doi:10.1029/2011lb008877.

[4] Mulia I.E., Asano T. Initial tsunami source estimation by inversion with an intelligent selection of model parameters and time delays // J. Geophys. Res.: Oceans. — 2016. — Vol. 121. — P. 441–456. doi:10.1002/jgrc.21401.

[5] Pires C.A.L., Miranda P.M. Tsunami waveform inversion by adjoint methods // J. Geophys. Res. — Vol. 106. — P. 19773–19796.

[6] Titov V.V., Gonzlez F.I., Bernard E.N., et al. Real-time tsunami forecasting: challenges and solutions // Nat. Hazards, Special Issue, U.S. National Tsunami Hazard Mitigation Program. — 2005. — Vol. 35, No. 1. — P. 41–58.

[7] Percival D.B., Denbo D.W., Eble M.C., et al. Extraction of tsunami source coefficients via inversion of DART® buoy data // Nat. Hazards. — 2011. — Vol. 58. — P. 567–590.

[8] DART® tsunameter retrospective and real-time data: a reflection on 10 years of processing in support of tsunami research and operations // Pure Appl. Geophys. — 2013. — Vol. 170, Iss. 9. — P. 1369–1384.

[9] Cheverda V.A., Kostin V.I. r-pseudoinverse for compact operator // Siberian Electronic Mathematical Reports. — 2010. — Vol. 7. — P. 258–282.

[10] Voronina T.A. Reconstruction of initial tsunami waveforms by a truncated SVD method // J. Inverse and Ill-posed Problems. — 2012. — Vol. 19. — P. 615–629.

[11] Voronin V.V., Voronina T.A., Tcheverda V.A. Inversion method for initial tsunami waveform reconstruction // Nat. Hazards Earth Syst. Sci. — 2015. — Vol. 15. — P. 1251–1263.

[12] Voronina T.A., Romanenko A.A. The new method of tsunami source reconstruction with r-solution inversion method // Pure Appl. Geophys. — 2016. — Vol. 173, Iss. 12. — P. 4089–4099.

[13] Voronina T.A., Tcheverda V.A., Voronin V.V. Some properties of the inverse operator for a tsunami source recovery // Sib. Electronic Math. Reports. — 2014. — Vol. 11. — P. 532–547.

[14] Satake K., Heidarzaden M. A review of source models of the 2015 Illapel, Chile earthquake and insights from tsunami data // Pure Appl. Geophys. — 2017. — Vol. 174, Iss. 1. — P. 1–9. doi:10.1007/s00024-016-1450-5.

[15] Marchuk An.G., Chubarov L.B., Shokin Yu.I. The Numerical Simulation of the Tsunami Wave. — Novosibirsk: Nauka, 1983.